Validation of Tomographic Measurement of Cerebral Blood Volume with C-11-Labeled Carboxyhemoglobin

M. E. Phelps, S. C. Huang, E. J. Hoffman, and D. E. Kuhl

University of California, Los Angeles, California

Red blood cells, tagged with C-11 by administration of ^{11}CO gas, have been used to portray the distribution of blood in the brain. To date, however, the accuracy of this approach has not been validated. We have performed in vitro measurements of regional cerebral blood volume (CBV) with red blood cells labeled with C-11 and Cr-51 in four dogs and two rhesus monkeys. These studies yielded a ratio of CBV_{C-11} to CBV_{Cr-51} of 1.02 ± 0.03 (s.d.) from 92 samples. A least-squares fit to these data showed $CBV_{C-11} = 1.01\ CBV_{Cr-51} + 0.037$; $P \ll 0.001$. The ratio of CBV in gray matter to that in white matter was 2.8 ± 0.4 ($n = 12$) and 3.1 ± 0.6 ($n = 8$). In vivo studies with emission computed tomography (ECT) and ^{11}CO-RBC gave coefficients of variation of ± 2.8% and ± 4.8% for cross-sectional CBV and regional (~4 cm^2) CBV over an 80-min period. The average human CBV was found to be 4.2 ± 0.4 cc blood per 100 g tissue. Clear tomographic delineation of the distribution of CBV in human subjects is achieved with ECT, which provides a "live" measurement of this parameter of cerebral hemodynamics. These data demonstrate that ^{11}CO administered by single-breath inhalation is a reliable and accurate blood tracer for measurement of CBV with ECT.

J Nucl Med 20: 328–334, 1979

Cerebral blood volume (CBV) is an important factor in the regulation and control of cerebral hemodynamics, and has been characterized in terms of normal values (*1–9*), its role in autoregulation (*6, 10–12*) and changes with P_aCO_2 and cerebral blood flow (*2, 3, 5, 6, 10, 13*). Changes in CBV have also been observed during generalized seizure (*14*), mental activity (*15*), and sleep (*16*). The tomographic study of CBV with emission computed tomography (ECT) has been used to demonstrate ischemia in and vasodilation around infarcted tissue (*17–19*); to assess alterations in CBV with head trauma (*19*), vasodilation in certain tumors (*6, 17*) and in regions surrounding subdural hematomas (*19, 20*); and to monitor reduction of CBV in cerebral edema followed by restoration with steroid therapy (*6*).

Received Sept. 29, 1978; revision accepted Nov. 21, 1978.

For reprints contact: Michael Phelps, Div. of Nuclear Medicine, Dept. of Radiology, School of Medicine, University of California, Los Angeles, Los Angeles, CA 90024.

The quantitative tomographic measurement of cerebral blood volume (CBV) was first performed by Kuhl et al. (*6*). These authors employed Tc-99m-labeled red blood cells (RBC) and a model developed by Phelps et al. (*21*) for x-ray fluorescence measurements of regional CBV. Phelps et al., Brownell et al., Muehllehner et al., and Ter-Pogossian et al. have used single-breath inhalation of ^{11}CO to label carboxyhemoglobin (^{11}CO RBC) and thus image the distribution of CBV (*22*). Glass et al. (*23*) have used ^{11}CO to measure the whole-body blood volume with a reported accuracy of ± 3% when rated against Cr-51 RBC. To date, however, no one has validated the tomographic measurement of CBV with ^{11}CO-RBC.

In the work reported here, in vitro studies were carried out in dogs and rhesus monkeys to compare regional CBV as measured by ^{11}CO RBC and Cr-51 RBC. Studies were also carried out in human subjects, following a single-breath inhalation of ^{11}CO

gas, to determine the accuracy and reproducibility of the in vivo tomographic measurement of CBV.

MATERIAL AND METHODS

Labeling of red blood cells. In the animal experiments, red blood cells were labeled in vitro with Cr-51 and in vivo with ^{11}CO. The Cr-51 labeling was carried out by withdrawing 20 ml of venous blood into a syringe containing 2 ml of acid citrate dextrose (ACD) solution and transferring this to a sterile evacuated bottle containing 75 μCi of [^{51}Cr] sodium chromate. This mixture was incubated for about 30 min with occasional swirling. Ascorbic acid, 50 mg in a 1-ml volume, was added to reduce the sodium chromate to Cr^{3+}. The solution was centrifuged, plasma discarded, and the red blood cells washed twice with saline. A 3-cc sample was taken for the measurement of unbound Cr-51, and the remainder was injected into the animal to measure CBV.

In the animal and human studies, red blood cells were labeled in vivo with ^{11}CO by administering an admixture of ^{11}CO and oxygen gases. The ^{11}CO was prepared by the $^{14}N(p,\alpha)^{11}C$ reaction as described elsewhere (*24*) and was >99% pure. In the animal studies, ^{11}CO was administered through a respirator that was used for controlled ventilation of the animals. In the human subjects, the individuals were allowed to take a deep breath from an embo bag containing ^{11}CO and O_2. The residual ^{11}CO was vented back into the bag and the subject returned to normal breathing of room air.

Animal experimental procedure. Four mongrel dogs weighing from 15 to 25 kg, and two rhesus monkeys weighing from seven to nine kg, were anesthetized with pentobarbital sodium (25 mg/Kg), paralyzed with gallium triethiodide, and passively ventilated on 100% oxygen with a Harvard respirator. Catheters were placed in the left and right saphonous leg veins for the injection of Cr-51 RBC and for removal of blood samples for counting and the measurement of hematocrit. A femoral-artery catheter was used to monitor arterial blood pressure and for the withdrawal of blood samples for the measurement of blood pH, P_aCO_2, and P_aO_2. The end-tidal PCO_2 was continuously monitored with capnograph*. Animals were given supplemental anesthesia as needed.

While breathing a mixture of ^{11}CO and O_2, the animals were injected with Cr-51 RBCs. Ten minutes were allowed for equilibration, five 6-cc blood samples were taken, and the animal was then killed by a rapid injection of concentrated KCl into the heart. The brain was rapidly excised and tissue separated into 2- to 4-g samples that were placed in weighed counting vials.

Three of the blood samples were also transferred to weighed counting vials. The tissue and blood samples were immediately counted for C-11 activity in a NaI(Tl) well counter. The vials were reweighed and the C-11 counting rate per gram of tissue (cpm/g) computed and decay-corrected to a common time. After the C-11 had decayed away, the samples were counted again to determine cpm/g for Cr-51. A spectrometer setting for the 511-keV radiation from C-11 was used to discriminate against the 320-keV Cr-51 gamma. No special effort was made to section tissue into the different anatomic components of the brain except for the samples of superficial cortex and subcortical white matter.

About 1 μCi of I-131-labeled serum albumin (RISA) was added to two of the blood samples taken after injection of the labeled RBCs, and also to a portion of the original Cr-51 RBC saline solution that was used for injection. These samples were centrifuged, RBCs and plasma separated, and each fraction counted for I-131, Cr-51, and C-11 with a Ge semiconductor detector to determine the distribution of C-11 and Cr-51 between RBCs and plasma. The RISA served to determine the amount of plasma trapped in the RBC fraction. These studies showed that less than 0.001% of the Cr-51 activity was in the saline phase of the Cr-51 RBC saline solution injected in the animals, and that less than 0.001% of the blood Cr-51 activity was in the plasma fraction at the time the animal was killed. The fraction of C-11 activity in the plasma was found to be less than 0.03% (value from ten samples; two samples had fractions of 1.1 and 0.9% but were disregarded because significant hemolysis was visually apparent).

Human experimental procedure†. Five male volunteers between the ages of 22 and 27 were administered 10–15 mCi of ^{11}CO by single-breath inhalation and tomographic studies were carried out with a positron transaxial tomograph† (*25*). Approximately 4 min were allowed for equilibration of ^{11}CO-RBC in the body blood pool. In two subjects a single tomographic plane was repeatedly imaged over a period of 80 min. The initial image was recorded for 2.0 min while the subsequent image times were progressively increased in proportion to the amount of C-11 decay (decay-compensation scanning mode) in order to accumulate an equal number of counts in each image. A 2-cc venous blood sample was taken at the mid time of each scan. These samples were transferred to weighed counting vials, counted in a well counter, reweighed, corrected for radioactive decay, and converted to cpm/g.

The tomograph was calibrated with each study by measuring the number of counts/unit time from

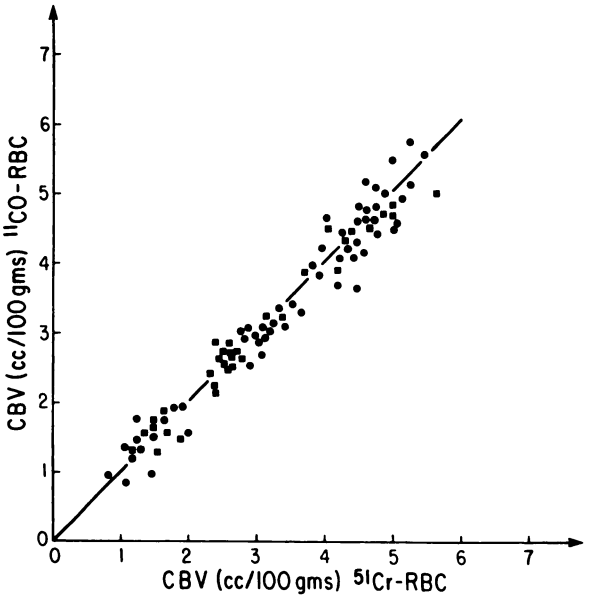

FIG. 1. Correlation of regional cerebral blood volumes measured in vitro with both ^{11}CO-RBC and Cr-51 RBC in four dogs and two rhesus monkeys. These data exhibit one-to-one correlation as described by Eq. 3. Each sample weighed from 2 to 4 g and was randomly excised throughout the brain without regard to anatomical identity, except for the 20 samples representing carefully separated superficial cortex and subcortical white matter. Circles and squares are from dog and monkey data, respectively. Solid line is from Eq. 3.

a uniform cylinder of positron activity (Ga-68). An aliquot of activity from the cylinder was also weighed and counted in the well counter to determine its cpm/g. The region-of-interest capabilities of the tomograph were then used to determine the cpm/cm² from the image of the uniform cylinder. These results were used to determine a calibration factor, f, between the tomograph and the well counter.

$$f = \frac{\text{cpm/cm}^2\text{ (tomog.)}}{\text{cpm/cc (well c.)}} \qquad (1)$$

The correction factor, human ^{11}CO-RBC brain images, and blood data allow the calculation of the regional CBV in units of cc blood per gram of tissue (see Eq. 2).

The medium-resolution mode (*25*) of the tomograph (1.3 cm FWHM) was used in all the studies reported in this work. The total number of counts in each image ranged from 600,000 to 900,000.

The procedure described above was also used in three other human subjects except that eight cross-sectional images from 7 cm above to 1 cm below the orbitomeatal plane were taken to image the distribution of CBV in the brain. These data were also used to calculate the average whole-brain CBV. Two-dimensional whole-body scans were also performed with the tomograph to display the general body distribution of blood. In these studies, three views of the subject (anteroposterior and two 60° obliques) are simultaneously recorded (*25*).

CBV model. The model for the measurement of regional cerebral blood volume (rCBV) is given in Refs. 6 and 21.

$$\text{rCBV (cc per 100 g)} = \frac{C_{T,i} \times 100}{C_B \times 0.85 \times d}, \qquad (2)$$

where $C_{T,i}$ is the blood tracer tissue concentration (cpm/cc) in region i, as determined by tissue counting in the in vitro experiments or as measured tomographically in the in vivo experiments. C_B is the venous blood concentration (cpm/cc) of the blood tracer, and d is the density of cerebral tissue (= 1.04 g/cc). The factor 0.85 corrects for the difference between the large-vessel and cerebral hematocrits (*21*), this factor being the average of the values from Everett et al. (*26*) in the rat, Larsen et al. (*27*) in man, Oldendorf et al. (*28*) in man, Sklar et al. (*29*) in the cat, and Studer et al. (*30*) in the rat namely, 0.85 ± 0.06 (1 s.d.). This value has been used routinely by Phelps et al. (*3, 10, 21*), Grubb et al. (*4, 5, 11, 12*), Kuhl et al. (*6, 19*), Eichling et al. (*31*), and Gado et al. (*14*).

The model responsible for Eq. 2 was used for both in vitro animal and in vivo human studies (in the animal experiments d is dropped from Eq. 2 since there $C_{T,i}$ is measured in units of cpm/g). In the animal studies, rCBV was measured with Cr-51 RBC and ^{11}CO-RBC to validate the use of ^{11}CO for

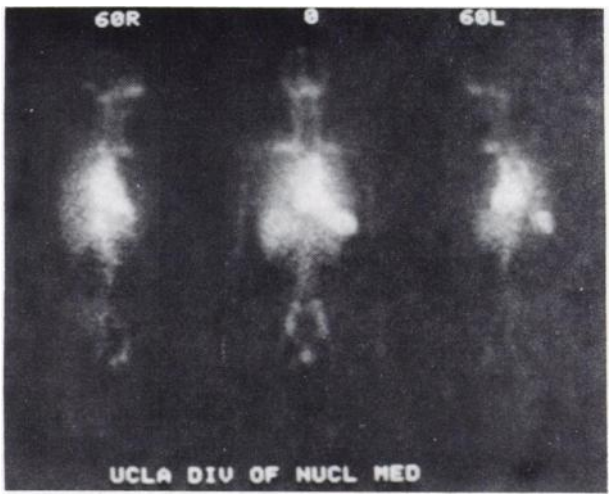

FIG. 2. Whole-body projections of blood distribution in human subject showing anteroposterior and two oblique views (± 60° apart). Ten mCi of ^{11}CO were administered by single-breath inhalation; total scan time for all three views was 20 min. Two-dimensional images show distribution of blood volume in body but have limited detail in any particular organ compared with tomographic images (Figs. 3, 5, and 6).

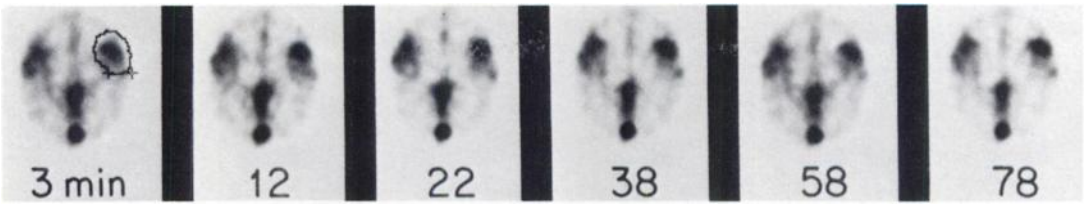

FIG. 3. Single cross section of head showing distribution of cerebral blood volume (CBV) with passage of time. Anterior is top, left is left, and level is 4 cm above orbitomeatal plane. Major features are high CBV in region of Sylvian fissure, straight sinus, superior sagittal sinus, and cortex. Numbers are mid-scan time in minutes. Images were selected from a total of ten taken over 80 min. Irregular dashed line shown at left is region of interest (ROI) selected for analysis of regional CBV. Note reproducibility and consistency of images (see Fig. 4).

the measure of CBV. In the human studies, rCBV and cross-sectional CBV values were repeatedly measured as functions of time to determine the reproducibility of the in vivo measurements in man.

RESULTS

Animal studies. The results for rCBV as measured with ^{11}CO-RBC are plotted against those measured with Cr-51 RBC in Fig. 1. These data were fitted with a linear least-squares analysis to yield the equation:

$$y = 1.01x + 0.037 \,(P \ll 0.001), \qquad (3)$$

where y and x are the rCBV values measured with ^{11}CO-RBC and ^{51}Cr-RBC, respectively. Table 1 summarizes the data from the individual animal experiments.

Figure 1 includes the data from samples considered to be anatomically isolated superficial cortex and subcortical white matter, and these results were analyzed separately to determine the CBV ratio of gray to white matter. The ratios were determined for each individual experiment to avoid differences produced by varying numbers of samples from individual animals that had different P_aCO_2 levels and therefore different values of cerebral blood flow and CBV. The average ratios of gray matter CBV to white matter CBV were 2.8 ± 0.4 (n = 12) and 3.1 ± 0.6 (n = 8).

Human studies. The general whole-body blood distribution is shown in the two-dimensional images of Fig. 2, whereas the cross-sectional distributions of CBV are shown in the tomographic images of Figs. 3, 5, and 6.

The reproducibility of the in vivo tomographic measure of CBV in a human subject is shown in Fig. 3. The same cross section was repeatedly imaged during 80 min. The numerical data for the average cross sectional CBV and a selected region of interest (Fig. 3, 3-min image) are plotted as a function of time in Fig. 4. The values for the average cross-sectional CBV in two individuals had a coefficient of variation of ± 2.8% (1 s.d.) for 10 images over an 80-min period in each individual. The average coefficient of variation over the 80-min time for eight different regions of interest (each ~4 cm²) in the two individuals was ± 4.5%.

The decay-corrected C-11 blood concentration was found to decrease with time. After the 3-min equilibration, the average biologic half-time for four human subjects was 195 ± 20 min.

The CBV at cross-sectional levels of the brain, from 7 cm above to 1 cm below the orbitomeatal line (Fig. 5), was calculated for three human subjects to determine the average total cerebral blood volume, which was found to be 4.2 ± 0.4 cc/100 g. This value includes the large-vessel and capillary blood. The average venous PCO_2 in these subjects was 42 ± 2 mm Hg.

DISCUSSION

The data in Fig. 1, Eq. 3, and Table 1 show a one-to-one correlation between CBV as measured with Cr-51 RBC administered intravenously and CBV from the administration of ^{11}CO by single-breath inhalation. These data show that the ^{11}CO-RBC method is reliable and accurate for the measurement of CBV.

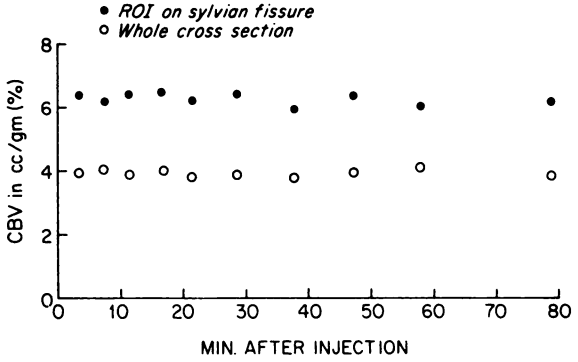

FIG. 4. Numerical values for CBV (from Eq. 2) in ROI shown in Fig. 3 (area of sylvian fissure), and in whole cross section, plotted as a function of time. Reproducibilities in human studies were ± 2.8% and ± 4.8%, respectively, for whole cross section and for ROI (≈ 4 sq. cm).

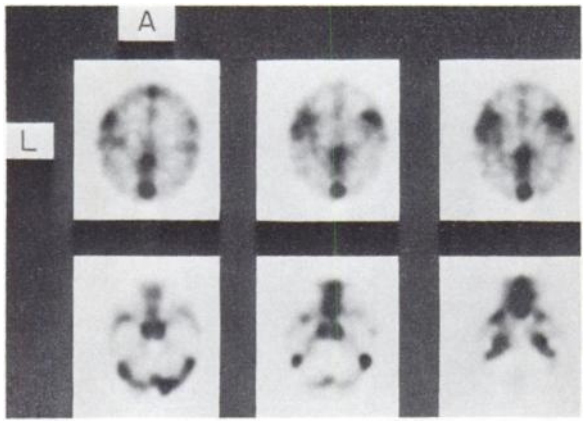

FIG. 5. Cerebral blood-volume distributions by tomograph in cross sections from human subject. Levels are from 7 cm above, to the orbitomeatal plane in one-cm increments, and proceed from left to right and top to bottom.

It was originally felt that because a small amount of CO is dissolved in plasma and is in equilibrium with red blood cells, CBV would be overestimated due to equilibration between plasma CO and tissue. This, however, was not found experimentally to be the case (Fig. 1, Eq. 3, Table 1). This is supported by the fact that the plasma fraction of C-11 activity was measured to be less than 0.03%, and if ^{11}CO was equilibrated with the extravascular space (~25 times the vascular) this would still only be about 1% of the ^{11}CO-RBC activity. The value of 1% is similar to the average overestimation of CBV by about 2% when ^{11}CO was compared with Cr-51 RBC (Table 1). However, the average 2% overestimation shown in Table 1 is not statistically significant. Glass et al. (*23*) reported that ^{11}CO overestimated whole-body blood volume by 5% because of binding to myoglobin. Since myoglobin does not occur in significant quantities in the brain, the error would be inconsequential.

The decrease in blood C-11 activity with time (biologic $t_{\frac{1}{2}}$ = 195 ± 20 min) is probably due to the slow equilibration with the low-flow compartments of the body, to slow expiration of ^{11}CO, and to some extraction by extravascular hemoglobin and myoglobin. Roughton and Root (*32*) report that no more than 60–70% of the CO that disappears from blood in the first hour is found in expired air. The remainder of the CO is reported by Wennesland et al. (*33*) to be extracted into the hemoglobin of red skeletal muscle and myoglobin of heart muscle. However, these studies were carried out at toxic levels (*32*) or at least with significant masses of CO (*33*), as opposed to the tracer levels of ^{11}CO used in our work, and therefore direct comparisons are of limited value. Glass et al. (*23*) have found, using ^{11}CO, that the whole-body blood volume is overestimated by about 5%, which is consistant with some retention in intravascular hemoglobin and myoglobin. This percentage, however, is considerably lower than would be predicted from the studies of Roughton and Root (*32*), and is lower than the measured values of Wennesland et al. (*33*) using relatively large masses of CO. Our value of 195 ± 20 min is in good agreement with the biologic half-time of 176 ± 50 reported by Glass et al. (*23*). The effect of the falling blood ^{11}CO concentration is removed in the CBV studies by taking several blood samples during the study (i.e., one during midtime of each scan).

Our values of 2.8 ± 0.4 and 3.1 ± 0.6, found in dog and monkey for the ratios of gray matter to white matter CBV, are of the same order as the ratio of gray to white cerebral blood flow of 3.8 (*34*) and capillary density of about 3 (*35*). Our in vitro ratios are considerably higher than the 1.4 and 1.8 found, respectively, by Greenberg et al. (*13*) and Kuhl et al. (*19*) in man using emission computed tomography. Because of spatial averaging in ECT, however, it would be expected that our in vitro values would be larger than those of the groups mentioned.

The average whole-brain CBV found in this work (4.2 ± 0.3 cc/100 g) is well within the range of values reported in the literature (Table 2). In spite of the diverse techniques used to measure CBV, we believe that the average basal CBV is about 4 cc/100 g.

The model for CBV is incorporated directly into tomograph software in such a manner that after the blood samples are counted and entered into the system, the images are converted to units of cc blood/g tissue. Our tomograph's region-of-interest (ROI) capability allows convenient extraction of

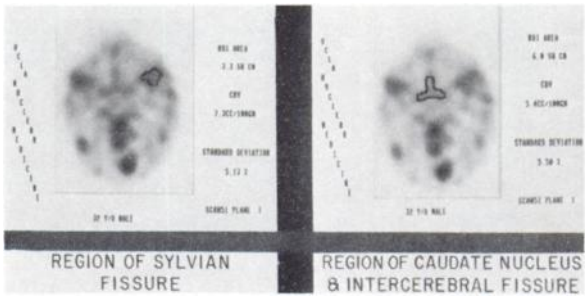

FIG. 6. Illustration of ROI extraction of regional CBV. Model represented in Eq. 2 is incorporated directly into software of tomograph, and once blood data are entered, regional values of CBV can be extracted for any region of interest (ROI) controlled by joy stick. Tomograph display provides cross-sectional image of CBV, selected ROI (regions outlined), numerical value of CBV, coefficient of variation within ROI, and cross-sectional area of ROI. As ROI is moved around image, these parameters are updated in real time.

TABLE 1. COMPARISONS OF CEREBRAL BLOOD VOLUME BY ^{11}CO-RBC AND Cr-51 RBC

Animal	No. of samples	CBV (^{11}CO-RBC) / CBV (^{51}Cr-RBC) (average ± 1 s.d.)	P_aCO_2 (mm Hg)	pH
Dog	13	0.98 ± 0.07	38	7.46
Dog	18	1.02 ± 0.08	42	7.43
Dog	13	1.05 ± 0.04	70	7.21
Dog	14	1.04 ± 0.05	36	7.47
Monkey	22	1.02 ± 0.08	49	7.38
Monkey	12	0.99 ± 0.07	38	7.45
Ave ± 1 s.d.	92	1.02 ± 0.03		

Average hematocrits of dogs and monkeys were 43.1 ± 1.2 and 39.9 ± 2.1.

TABLE 2. IN VIVO VALUES OF CEREBRAL BLOOD VOLUME (CBV)* IN THE NORMAL BRAIN

Authors	Animal	Average CBV (cc/100 g)
Grubb et al. (*4*)	Man	3.2
Phelps et al. (*3*)	Monkey	5.4 ± 0.6†
Smith et al. (*2*)	Goat	4.8 (4.1)‡
Grubb et al. (*10*); Eichling et al. (*31*)	Monkey	3.6 ± 0.5
Kuhl et al. (*6*)	Baboon	3.3 ± 0.7
Greenberg et al. (*11*)	Human	4.3
Mathew et al. (*7*)	Human	4.2
Penn et al. (*8*)	Human	3.0
Ladurner et al. (*9*)	Human	5.7 (cortex) 5.1 (thalamus)
Kuhl et al. (*19*)	Human	4.34 ± 0.50‖
This work	Human	4.2 ± 0.4

* CBV values at basal PCO_2 of about 36–43 mm Hg. Average values for whole brain unless otherwise noted.

† Regional value in frontal lobe.

‡ Value in parenthesis is the authors' value corrected for the cerebral hematocrit which is 0.85 of large-vessel value (*21*).

‖Average value from cross-sectional levels from about 2 to 5 cm above orbitomeatal plane.

CBV values, as shown in Fig. 6. As the ROI is moved around the image, the area of the ROI, the CBV, and coefficient of variation within the ROI are updated in real time.

The whole-body images (Fig. 2) provide an overall perspective of the body's blood distribution, but they lack the spatial detail and quantitative features of the tomographic approach.

The quantitative regional tomographic measurement of CBV in human subjects is seen to be reproducible (Figs. 3 and 4) and allows clear delineation of the distribution of cerebral blood (Fig. 5) by a noninvasive technique. Similar reproducibility in the measurement of CBV with emission computed tomography and Tc-99m RBC has been reported by Kuhl et al. (*6*). Note, further, that the measurement of CBV is essentially a "live" measurement, since observed temporal changes in CBV can produce concomitant changes in the tissue concentration of the blood tracer (i.e., measured CBV). Thus sequential tomograms of CBV from a single administration of ^{11}CO allow one to observe and measure the response of this variable to induced or naturally occurring changes in the hemodynamics of the brain.

FOOTNOTES

* Beckman LB-50, Beckman Instruments, Fullerton, CA

† All human studies were carried out under approval of the UCLA School of Medicine human use committee.

‡ "ECAT," ORTEC, Inc., Oak Ridge, TN

ACKNOWLEDGMENTS

This work was partially supported by DOE Contract EY-76-C-03-0012 Gen-12 and NIH Grant 7Ro1-GM 24839-01.

REFERENCES

1. Nylin G, Hedlund S, Regnstrom O: Studies of the cerebral circulation with labeled erythrocytes in healthy man. *Circ Res* 9: 664–674, 1961
2. Smith AL, Neufeld GR, Ominsky AJ, et al: Effect of arterial CO_2 tension on cerebral blood flow, mean transit time, and vascular volume. *J Appl Physiol* 31: 701–707, 1971
3. Phelps ME, Grubb RL, Ter-Pogossian MM: Correlation between Pa_{CO_2} and regional cerebral blood volume by X-ray fluorescence. *J Appl Physiol* 35: 274–280, 1973
4. Grubb RL, Phelps ME, Ter-Pogossian M: Regional cerebral blood volume in humans. *Arch. Neurol.* 28: 38–44, 1973
5. Grubb RL, Raichle ME, Eichling JO, et al: The effects of changes in $PaCO_2$ on cerebral blood volume, blood flow, and vascular mean transit time. *Stroke* 5: 630–639, 1974
6. Kuhl DE, Reivich M, Alavi A, et al: Local cerebral blood volume determined by three-dimensional reconstruction of radionuclide scan data. *Circ Res* 36: 610–619, 1975
7. Mathew NJ, Meyer JS, Bell RL, et al: Regional cerebral blood flow and blood volume with the gamma camera. *Neuroradiology* 4: 133–140, 1972
8. Penn Rd, Walser R, Ackerman L: Cerebral blood volume in man. Computer analysis of computerized brain scan. *JAMA* 234: 1154–1155, 1975
9. Ladurner G, Zilkha E, Iffif LD, et al: Measurement of regional cerebral blood volume by computerized axial tomography. *J Neurol Neurosurg Psychiatry* 39: 152–158, 1976
10. Phelps ME, Grubb RL, Raichle ME, et al: Correlation of regional cerebral blood volume with $PaCO_2$ and arterial blood pressure. In: *Cerebral Circulation and Metabolism.* Langfitt T, McHenry L, Reivich M, et al, eds. New York, Springer-Verlag, 1975, pp 24–26
11. Grubb RL, Phelps ME, Raichle ME, et al: The effects of arterial blood pressure on the regional cerebral blood volume by x-ray fluorescence. *Stroke* 4: 390–399, 1973
12. Grubb RL, Raichle ME, Phelps ME, et al: Effects of increased intercranial pressure on cerebral blood volume, blood flow, and oxygen utilization in monkeys. *J Neurosurg* 43: 385–398, 1975

13. GREENBERG J, ALAVI A, REIVICH M, et al: Local cerebral blood volume response to carbon dioxide in man. *Circ Res* 43: 324–331, 1978
14. GADO MH, PHELPS ME, HOFFMAN EJ, et al: Changes in cerebral blood volume and vascular mean transit time during induced cerebral seizures. *Radiology* 121: 105–109, 1976
15. RISBERG J, INGVAR DH: Regional changes in cerebral blood volume during mental activity. *Expt Brain Res* 5: 72–78, 1968
16. RISBERG J, GUSTAVSSON K. INGVAR DH: Regional cerebral blood volume during paridoxical sleep. In: *Cerebral blood flow: Clinical and experimental results*. Brock M, Fieshi C, Ingvar DH et al, eds. Springer-Verlag, Berlin, 1969, pp 101–103
17. PHELPS ME, HOFFMAN EJ, COLEMAN RE, et al: Tomographic images of blood pool perfusion in brain and heart. *J Nucl Med* 17: 603–612, 1976
18. ACKERMAN RH, CORREIA JA, ALPERT NM, et al: Positron imaging as a clinical tool for demonstrating disturbed cerebral circulation and metabolism. *J Comput Tomog* 2: 664, 1978 (abst)
19. KUHL DE, ALAVI A, HOFFMAN E, et al: Local cerebral blood volume in head injured patients: determination by emission computed tomography of (Tc-99m) red cells. *J Nucl Med* 19: 699–700, 1978 (abst)
20. KUHL DE, EDWARDS RQ, RICCI AR, et al: The MARK IV system for radionuclide computed tomography of the brain. *Radiology* 121: 405–413, 1976
21. PHELPS ME, GRUBB RL, TER-POGOSSIAN MM: In vivo cerebral blood volume by X-ray fluorescence: validation of the method. *J Appl Physiol* 35: 741–747, 1973
22. PHELPS, ME: Emission computed tomography. *Sem Nucl Med* 7: 337–365, 1977
23. GLASS H, BRANT A, CLARK JC, et al: Measurement of blood volume using red cells labeled with radioactive carbon monoxide. *J Nucl Med* 9: 571–575, 1968
24. CLARK, JC, BUCKINGHAM PD: Short-lived radioactive gases for clinical use. London and Boston, Butterworths, 1975, pp 227–231
25. PHELPS ME, HOFFMAN EJ, HUANG SC, et al: ECAT: A new computerized tomographic imaging system for positron-emitting radiopharmaceuticals. *J Nucl Med* 19: 635–647, 1978
26. EVERETT NB, SIMMONS B, LASHER EP: Distribution of blood (Fe^{59}) and plasma (I^{131}) volumes of rats determined by liquid nitrogen freezing. *Circ Res* 4: 419–424, 1956
27. LARSEN OA, LASSEN NA: Cerebral hematocrit in normal man. *J Appl Physiol* 19: 571–574, 1964
28. OLDENDORF WH, KITANO M, SHIMIZU S, et al: Hematocrit of the human cranial blood pool. *Circ Res* 17: 532–539, 1965
29. SKLAR FH, BURKE EF, JR, LANGFITT TW: Cerebral blood volume: values obtained with ^{51}Cr-labeled red blood cells and RISA. *J Appl Physiol* 24: 78–82, 1968
30. STUDER R, POTCHEN EJ: The radioisotopic assessment of regional microvascular permiability of macromolecules. *Microvasc Res* 3: 35–48, 1971
31. EICHLING JO, RAICHLE ME, GRUBB RL, JR, et al: In vivo determination of cerebral blood volume with radioactive oxygen-15 in the monkey. *Circ Res* 37: 707–714, 1975
32. ROUGHTON RJW, ROOT WS: The fate of CO in the body during recovery from mild carbon monoxide poisoning in man. *Am J Physiol* 145: 239–252, 1945
33. WENNESLAND R, NOMOF N, BROWN E, et al: Distribution of CO and radiochromium in blood and tissue of rabbit and dog. I. Carbon monoxide. *Proc Soc Exper Biol Med* 96: 655–657, 1957
34. INGVAR ND, CRONQVIST S, EKBERG R, et al: Normal values of regional cerebral blood flow in man, including flow and weight estimates of grey and white matter. In *Regional Cerebral Blood Flow*. Ingvar DH, Lassen NA, eds. Copenhagen, Munksgaard, 1965, pp 72–78
35. LIERSE W, HORSTMANN E: Quantitative anatomy of the cerebral vascular bed with special emphasis on homogeneity and inhomogeneity in small parts of the grey and white matter. In *Regional Cerebral Blood Flow*. Ingvar DH, Lassen NA, eds. Copenhagen, Munksgaard, 1965, pp 15–19